

## Seeded-Growth Approach to Selective Metallization of Microcontact-Printed Patterns

Agnes A. Mewe, E. Stefan Kooij,\* and Bene Poelsema

University of Twente, MESA+ Institute for Nanotechnology, P.O. Box 217,  
7500 AE Enschede, The Netherlands

Received November 4, 2005. In Final Form: April 12, 2006

We report on a versatile nanocolloidal route to obtain large-scale conducting metal microstructures on a silicon oxide substrate. By using microcontact printing of an aminosilane, we create functionalized regions on the silicon oxide surface onto which gold nanoparticles selectively adhere. By using an established electroless, seeded-growth process, the individual, isolated gold nanocrystals are enlarged past the percolation threshold to form conducting metal structures. Quantitative characterization of metal coverage, thickness, and roughness has been performed with scanning electron microscopy and spectroscopic ellipsometry.

### Introduction

Well-defined metallic micro- and nanostructures on a variety of substrates are of special interest for wiring of electronic devices, for example, solar cells. Also, other electronic applications, such as display technology, may benefit from a reproducible, versatile, cost-efficient, and environmentally favorable metal deposition technique.

The conventional procedure to fabricate structures with sizes down into the submicron range is based on resist patterning of a substrate (by photolithography and, more recently, by microcontact printing) in combination with several curing, etching, and washing steps.<sup>1,2</sup> Despite its enormous impact on IC technology, this top-down approach has a number of disadvantages. The consequence of the etching procedure is a considerable waste of material because a large amount of the deposited metal film is removed. A recycling system to regain the metal ions from the etch solution is expensive and time-consuming. Another problem is the use of chemicals for etching: they are in general environmentally unfriendly and methods to avoid their use should be pursued.

Here, we present a promising alternative to the aforementioned existing structuring methods, without the disadvantageous consequences of lithographic patterning and etching. In a combination of bottom-up and top-down approaches, we employ the selective self-assembly of nanocolloidal metal particles from solution at chemically patterned surfaces. These particles provide catalytic binding sites for subsequent site-selective metal deposition.

Although we demonstrate the procedure for adsorption of gold particles on silicon oxide surfaces, in principle, it can be extended to any combination of particle and substrate, provided a sufficiently high contrast in surface affinity can be achieved by chemical functionalization and selective growth is catalyzed by the nanoparticles. With respect to chemical patterning, existing work has primarily been concentrated on the system of (alkane)-thiols on gold, as these molecules adsorb in well-ordered monolayers.<sup>1–10</sup> Adsorption of functional molecules (silanes) on silicon can easily result in disordered mono- or multilayers,

as the molecules hydrolyze in the presence of water, enabling undesired polymerization.<sup>11,12</sup> However, we will show that these molecules can be used effectively for chemical patterning. The low working temperature of this procedure and the electroless nature of the deposition process allow plastics to be involved as substrates and, therefore, open the way to flexible devices.

### Experimental Section

SEM measurements were performed on a LEO 1550 FEG SEM. Spectroscopic ellipsometry was performed on a Woollam VASE system, equipped with the WVASE32 software package for determination of film thickness and surface roughness.

Gold nanoparticles with a diameter of 13 nm were prepared using standard citrate reduction procedures, as described previously.<sup>16,17</sup> Polished silicon wafers with varying oxide thickness were cleaved into 15 × 15 mm<sup>2</sup> pieces. A high surface affinity for the colloidal gold particles was achieved by derivatization of the substrates in a 10% v/v (aminopropyl)triethoxysilane (APTES) in methanol solution, as described by Kooij et al.<sup>17</sup> By using the adsorbed, isolated gold nanocrystals on the substrate as seeds, we performed electroless deposition of silver in a solution of 2.24 M NH<sub>3</sub>, 0.56 M CH<sub>3</sub>COOH, 0.1 M NH<sub>2</sub>NH<sub>2</sub> (hydrazine), and 3.2 mM AgNO<sub>3</sub>, following a recipe of Tong et al.<sup>13</sup> Electroless deposition of gold is done by immersion

(3) Loo, Y.-L.; Lang, D. V.; Rogers, J. A.; Hsu, J. W. P. *Nano Lett.* **2003**, *3*, 913.

(4) Geissler, M.; Wolf, H.; Stutz, R.; Delamarche, E.; Grummt, U.-W.; Michel, B.; Bietsch, A. *Langmuir* **2003**, *19*, 6301.

(5) Losic, D.; Shapter, J. G.; Gooding, J. J. *Electrochem. Commun.* **2001**, *3*, 722.

(6) Michel, B.; Bernard, A.; Bietsch, A.; Delamarche, E.; Geissler, M.; Juncker, D.; Kind, H.; Renault, J.-P.; Rothuizen, H.; Schmid, H.; Schmidt-Winkel, P.; Stutz, R.; Wolf, H. *IBM J. Res. Dev.* **2001**, *45*, 697.

(7) He, H. X.; Zhang, H.; Li, Q. G.; Zhu, T.; Li, S. F. Y.; Liu, Z. F. *Langmuir* **2000**, *16*, 3846.

(8) Böhm, I.; Lampert, A.; Buck, M.; Eisert, F.; Grunze, M. *Appl. Surf. Sci.* **1999**, *141*, 237.

(9) Delamarche, E.; Schmid, H.; Bietsch, A.; Larsen, N. B.; Rothuizen, H.; Michel, B.; Biebuyck, H. *J. Phys. Chem. B* **1998**, *102*, 3324.

(10) Larsen, N. B.; Biebuyck, H.; Delamarche, E.; Michel, B. *J. Am. Chem. Soc.* **1997**, *119*, 3017.

(11) Halliwell, C. M.; Cass, A. E. G. *Anal. Chem.* **2001**, *73*, 2476.

(12) Fontaine, P.; Goldmann, M.; Rondelez, F. *Langmuir* **1999**, *15*, 1348.

(13) Tong, H.; Zhu, L.; Li, M.; Wang, C. *Electrochim. Acta* **2003**, *48*, 2473.

(14) Musick, M. D.; Pena, D. J.; Botsko, S. L.; McEvoy, T. M.; Richardson, J. N.; Natan, M. J. *Langmuir* **1999**, *15*, 844.

(15) Brown, K. R.; Lyon, L. A.; Fox, A. P.; Reiss, B. D.; Natan, M. J. *Chem. Mater.* **2000**, *12*, 314.

(16) Frens, G. *Nature* **1973**, *241*, 20.

(17) Kooij, E. S.; Wormeester, H.; Brouwer, E. A. M.; van Vroonhoven, E.; van Silfhout, A.; Poelsema, B. *Langmuir* **2002**, *18*, 4401.

\* Corresponding author. E-mail: e.s.kooij@utwente.nl. Telephone: +31 53 489 3146. Fax: +31 53 489 1101.

(1) Libioulle, L.; Bietsch, A.; Schmid, H.; Michel, B.; Delamarche, E. *Langmuir* **1999**, *15*, 300.

(2) Kumar A.; Biebuyck, H. A.; Whitesides, G. M. *Langmuir* **1994**, *10*, 1498.

of the gold-seeded substrates in a solution of 0.3 mM HAuCl<sub>4</sub> and 0.4 mM NH<sub>2</sub>OH, following a previously reported procedure.<sup>14,15</sup>

The stamp material for microcontact printing, poly(dimethylsiloxane) (PDMS, Sylgard 184) is cured on a lithographically patterned silicon master for 4 h at 60 °C. A drop of “ink”, containing 1% v/v functional molecules, is placed on the stamp, rinsed with solvent (either methanol or ethanol) after 30 s, and dried in a nitrogen flow. The stamp is placed on the substrate, pressed gently to ensure conformal contact, and after typically a few seconds, removed carefully to avoid distortion of the printed pattern.

*N*-(2-aminoethyl)-11-aminoundecyltrimethoxysilane (AEUTS) was obtained from Gelest (Tullytown, PA). Hydrazine and acetic acid were obtained from Acros. All other chemicals, including (aminopropyl)triethoxysilane (APTES), were obtained from Merck.

### Bottom-Up Metal Deposition: Self-Assembly and Electroless Deposition

First, we will describe and characterize substrates that are homogeneously covered with gold nanoparticles. In the next section, we will then describe the patterning step.

Gold nanoparticles with a diameter of 13 nm, as described in the experimental part, were used as seeds for metal deposition. Because both the citrate-stabilized gold nanoparticles in solution and the silicon oxide surface are negatively charged, giving rise to repulsive electrostatic forces, adsorption of particles requires the use of an intermediate compound. For functionalization, we immerse the silicon oxide surface into a solution of an aminosilane, in this case, 10% v/v APTES in methanol. APTES is a frequently used functional molecule.<sup>17–20</sup> The silane end-group hydrolyzes and forms a covalent bond to the oxide layer of the substrate.<sup>12,21</sup> The amine end-group not only provides a short-range attractive interaction with the citrate molecules, but also has a high affinity for gold and will cause irreversible adsorption of the gold nanoparticles in this experimental setup.<sup>17,19</sup>

The self-assembly of gold nanocolloidal particles generally gives rise to isolated gold particles. Their mutual distance is determined by the spatial extent of the repulsive interaction arising from the surface charge on the nanocolloidal particles. To obtain a percolated layer of metal clusters, an electroless metal deposition process can be applied in which the gold nanoparticles act as a seed layer.<sup>14,15,22</sup>

We use spectroscopic ellipsometry for optical characterization of the metal films. This versatile, nondestructive technique enables accurate assessment of the optical properties in both ex situ and in situ measurements. Figure 1 shows the ellipsometry spectra of a gold nanoparticle-covered silicon oxide surface (dotted line) prior to growth, and the spectra after electroless deposition for 2 min, 5 min, and 10 min, corresponding to three different amounts of silver. Also shown are the corresponding SEM images of the silver layer morphology, revealing the transition to a percolated state. The ellipsometry spectra of the gold nanoparticle film before growth exhibit strong oscillations due to the 200-nm silicon oxide layer.

Upon electroless silver deposition, these oscillations gradually disappear, indicating the formation of a nontransparent silver layer. Similar experiments on considerably thinner oxide layers reveal the disappearance of the gold plasmon resonance and large changes in the optical response in the low-energy region

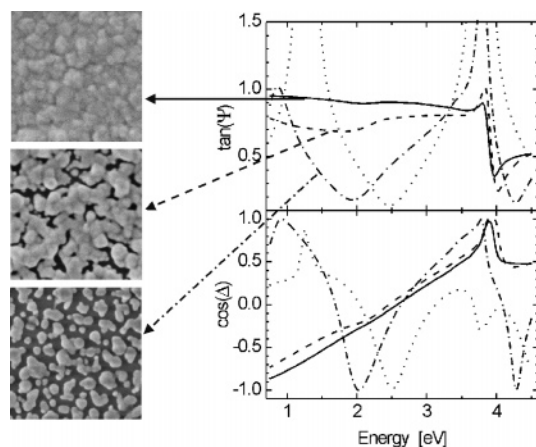


**Figure 1.** Ellipsometry spectra of a 200-nm silicon oxide layer on a silicon substrate after adsorption of a monolayer of gold nanoparticles (dotted lines), and after subsequent electroless silver deposition for 2 min (dash-dotted lines), 5 min (dashed lines), and 10 min (solid lines). The SEM images on the left (500 × 500 nm<sup>2</sup>) show the growth morphology, corresponding to the ellipsometry spectra, as indicated.

of the spectra, which we ascribe to the emergence of Drude-like behavior as the percolation threshold is passed. The SEM images in Figure 1 indeed confirm the evolution from isolated clusters to a closed layer. Model calculations, using the ellipsometry software, are also in agreement with this observation. For the spectra corresponding to the upper image in Figure 1, we find a silver layer thickness of approximately 65 nm, while the spectra related to the lowest image can only be described by considering a nonclosed layer.

To assess the macroscopic conductivity of the layers after different silver deposition times, we performed four-point probe electrical measurements on the substrates of Figure 1. The results reveal that conductance only starts when the particles coalesce, as is to be expected. The sample with the enlarged, but still isolated clusters shows no measurable conductance. Measurements on samples with a thicker silver layer (100–120 nm) show an average specific resistivity of  $(3.1 \pm 0.2) \times 10^{-8} \Omega\text{m}$ , approximately twice the literature bulk value of  $1.59 \times 10^{-8} \Omega\text{m}$ . A thick layer of 100 nm has been modeled with an 80-nm full silver layer plus a 20-nm effective medium approximation (EMA) consisting of 90% silver. The EMA provides an indication of the actual roughness. A slightly further decrease in resistivity is expected for thicker layers, but we cannot confirm this, as ellipsometry does not give a reliable fit for thick silver layers. The higher resistivity as compared to the bulk value is most likely related to: (i) the limited grain size in the films due to the deposition method and the use of seeds, (ii) the probably high grain boundary reflection coefficient, due to the use of two different metals (gold and silver) and the deposition technique,<sup>23</sup> and (iii) the presence of organic contaminants. By conventional deposition techniques such as evaporation, electroplating, and sputtering, resistivities of 1.1–1.2 times the bulk value can be achieved.<sup>23,24</sup>

We have chosen silver as deposition material because its intrinsic electrical conductance is higher than that of gold. Still, the electroless deposition of gold is interesting to investigate because we expect that, in this case, grain boundaries will have less influence on the conductivity. This implies that conductance

(18) Zheng, J.; Zhu, Z.; Chen, H.; Liu, Z. *Langmuir* **2000**, *16*, 4409.

(19) Kooij, E. S.; Brouwer, E. A. M.; Wormeester, H.; Poelsma, B. *Langmuir* **2002**, *18*, 7677.

(20) Choi, K. H.; Bourgojn, J. P.; Auvray, S.; Esteve, D.; Duesberg, G. S.; Roth, S.; Burghard, M. *Surf. Sci.* **2003**, *462*, 195.

(21) Vrancken, K. C.; Possemiers, K.; van der Voort, P.; Vansant, E. F. *Colloids Surf., A* **1995**, *98*, 235.

(22) Meltzer, S.; Resch, R.; Koel, B. E.; Thompson, M. E.; Madhukar, A.; Requicha, A. A. G.; Will, P. *Langmuir* **2001**, *17*, 1713.

(23) Zhang, W.; Brongersma, S. H.; Richard, O.; Brijis, B.; Palmans, R.; Froyen, L.; Maex, K. *Microelectron. Eng.* **2004**, *76*, 146.

(24) Manepalli, R.; Stepniak, F.; Bidstrup-Allen, S. A.; Kohl, P. A. *IEEE Trans. Adv. Packag.* **1999**, *22*, 4.



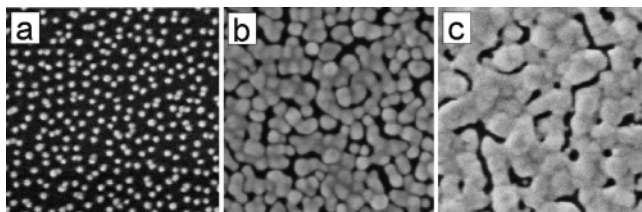


**Figure 2.** Gold nanoparticles on a silicon oxide surface, (a) as-deposited, (b) after 5 min electroless deposition of gold, (c) after 5 min electroless deposition of silver. Image size  $500 \times 500 \text{ nm}^2$ .

will be achieved for a thinner metal layer. Indeed, we experimentally determined for a gold thickness of only 60 nm a resistivity value of approximately  $4.2 \times 10^{-8} \Omega\text{m}$ , less than twice the bulk value of  $2.21 \times 10^{-8} \Omega\text{m}$ . However, the gold deposition proceeds much more slowly, it results in inhomogeneous coverage, and the procedure is very sensitive to glassware contamination. We observe a different morphology for electroless gold deposition compared to silver, as is clearly shown in Figure 2b and 2c. It shows that the originally isolated gold particles are isotropically enlarged. The coalescence of many particles, indicating the onset of percolation, is clearly visible. The regions with connected particles have a metal-like appearance by eye, in contrast to substrates on which the as-deposited gold particles lie isolated on the surface.

### Top-Down Patterning: Microcontact Printing

As mentioned before, gold nanoparticles only adsorb on functionalized silicon oxide substrates. Self-assembly of gold nanocrystals in patterns can therefore be accomplished by locally functionalizing the substrate. Several techniques have been described to chemically pattern various substrates. They include direct printing techniques, such as microcontact printing ( $\mu\text{CP}$ ),<sup>2,6,25</sup> microtransfer molding ( $\mu\text{TM}$ ),<sup>26</sup> dip pen nanolithography (DPN),<sup>27,28</sup> and nano-imprint lithography (NIL),<sup>29</sup> but other methods have also been reported in which a homogeneously functionalized surface is locally “defunctionalized” by using an AFM tip<sup>18,30</sup> or by microcontact printing.<sup>31</sup> In microcontact printing, feature sizes of typically  $1 \mu\text{m}$  are easily obtained, while the substrate dimensions are well up-scalable to wafer size and the patterning method is fast (on the order of seconds).<sup>32–34</sup> Because of the elastomeric properties of the stamp, this simple and low-cost technology is applicable to flat as well as curved surfaces,<sup>35</sup> resulting in a very competitive structuring tool.

We applied microcontact printing of the aforementioned APTES molecules on the silicon oxide substrates, as this molecule has proven to be a good intermediate compound. However, we observed no strictly selective deposition of particles in the regions of conformal contact. Instead, a background density of particles is present in the noncontacted regions, indicating that also on

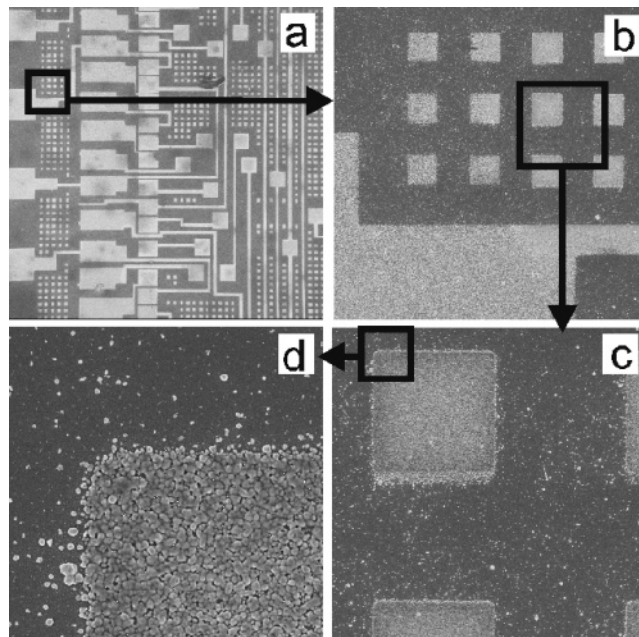


**Figure 3.** Chemically patterned substrates after gold nanoparticle adsorption and 5 min electroless deposition of silver. The image sizes are: (a)  $1 \times 1 \text{ mm}^2$ , (b)  $100 \times 100 \text{ mm}^2$ , (c)  $25 \times 25 \text{ mm}^2$ , (d)  $4 \times 4 \text{ mm}^3$ .

these sites there is still a sufficient surface concentration of amine-groups to bind a number of gold nanocrystals. We determined that this background density was approximately one-half of the density of the contacted area. Because there is a distinct border between high and low nanoparticle density, we assume that the background of particles is due to the presence of APTES molecules in the gas phase. If surface diffusion would be dominant, a sharp border between stamped and nonstamped regions is not expected.<sup>36</sup> APTES molecules are present in the gas phase due to their relatively low molecular weight, leading to a high vapor pressure. As a result, a considerable amount of molecules from the gas phase will be deposited on the silicon surface, enabling gold particle adsorption on the noncontacted regions.

To verify our assumption that APTES in the gas-phase accounts for the presence of nanoparticles on the noncontacted regions, we applied microcontact printing using AEUTS, a molecule with identical functional groups as APTES, but with a higher molecular weight. We expect the vapor pressure to be lower and that the AEUTS gas phase is sufficiently suppressed to obtain deposition only in the contacted regions. In literature, an inking concentration of  $<1 \text{ mM}$  is frequently used for long molecules, mostly for thiols,<sup>7,9,37,38</sup> but also concentrations of  $10\text{--}100 \text{ mM}$  give good results.<sup>5</sup> We use a concentration of  $30 \text{ mM}$  AEUTS in ethanol. The result of microcontact printing with this solution and subsequent gold nanocrystal adsorption is shown in Figure 3. The SEM images in Figure 3 are taken after electroless silver deposition, showing that the silver deposition is selective enough to prevent undesired metal connections. They indicate a high selectivity of amine functionalization and nanoparticle deposition. A high density of particles is observed in the regions of conformal contact, while the regions where the polymeric stamp did not touch the substrate are nearly particle-free (we counted on average eight nanoparticles per  $\mu\text{m}^2$ ). This implies that the amine

(25) Pompe, T.; Ferry, A.; Herminghaus, S.; Kriele, A.; Lorenz, H.; Kotthaus, J. P. *Langmuir* **1999**, *15*, 2398.

(26) Bailey, R. C.; Stevenson, K. J.; Hupp, J. T. *Adv. Mater.* **2000**, *12*, 1930.

(27) Piner, R. D.; Zhu, J.; Xu, F.; Hong, S.; Mirkin, C. A. *Science* **1999**, *283*, 661.

(28) Wang, X.; Ryu, K. S.; Bullen, D. A.; Zou, J.; Zhang, H.; Mirkin, C. A.; Liu, C. *Langmuir* **2003**, *19*, 8951.

(29) Lee, H.; Jung, G.-Y. *Microelectron. Eng.* **2005**, *77*, 42.

(30) Li, Q.; Zheng, J.; Liu, Z. *Langmuir* **2003**, *19*, 166.

(31) Geissler, M.; Kind, H.; Schmidt-Winkel, P.; Michel, B.; Delamar, E. *Langmuir* **2003**, *19*, 6283.

(32) Rogers, J. A.; Nuzzo, R. G. *Mater. Today* **2005**, *8*, 50.

(33) Decré, M. M. J.; Schneider, R.; Burdinski, D.; Schellekens, J.; Saalmink, M.; Dona, R. *Mater. Res. Soc. Symp. Proc.* **2004**, *EXS-2*, M4.9.

(34) Schellekens, J.; Burdinski, D.; Saalmink, M.; Beenhakkers, M.; Gelinck, G.; Decré, M. M. J. *Mater. Res. Soc. Symp. Proc.* **2004**, *EXS-2*, M2.9.

(35) Hidber, P. C.; Helbig, W.; Kim, E.; Whitesides, G. M. *Langmuir* **1996**, *12*, 1375.

(36) Sharpe, R. B. A.; Burdinski, D.; Huskens, J.; Zandvliet, H. J. W.; Reinhoudt, D. N.; Poelsema, B. *Langmuir* **2004**, *20*, 8646.

(37) Geissler, M.; Wolf, H.; Stutz, R.; Delamar, E.; Grummt, U.-W.; Michel, B.; Bietsch, A. *Langmuir* **2003**, *19*, 6301.

(38) Rozlosnik, N.; Gerstenberg, M. C.; Larsen, N. B. *Langmuir* **2003**, *19*, 1182.

functionalization (i.e., AEUTS molecules) is only present on the surface where there has been conformal contact. These results strongly indicate that the desorption rate of the AEUTS from the wells of the stamp is much lower than that for APTES, in accordance with its assumed lower vapor pressure, as mentioned earlier. Correspondingly, adsorption from the gas phase as observed with APTES is largely inhibited, which leads to well-defined printed patterns with sharp edges.

We also verified whether the presence of gold nanoparticles is necessary to catalyze the electroless deposition of silver. On a homogeneously amine-functionalized surface without gold nanoparticles, silver reduction only occurs in a very limited way, not contributing to the formation of conducting structures.

### Conclusion

We have introduced a versatile method that enables the formation of chemically patterned micron-sized structures on silicon oxide substrates on a large scale by microcontact printing

of an aminosilane. Metallization is achieved by selective gold nanoparticle adsorption and subsequent electroless metal deposition. After sufficient metal deposition, we obtain highly conductive films: a silver layer thickness of 100 nm and a gold layer of 60 nm reach specific resistivities of approximately twice the bulk value. Metal bulk behavior was confirmed by ellipsometry measurements, showing dominant low-energy Drude features.

**Acknowledgment.** We thank Cora Salm and Eddy Ruiters for their help in performing the conductivity measurements. We also thank Ruben Sharpe and Jurriaan Huskens for helpful discussions. This research is supported by the Technology Foundation STW, and is part of the research program of the Stichting voor Fundamenteel Onderzoek der Materie (FOM), financially supported by the Nederlandse Organisatie voor Wetenschappelijk Onderzoek (NWO).

LA052968K